A dynamic river network method for the prediction of floods using a parsimonious rainfall-runoff model

Aynalem Tassachew Tsegaw, Thomas Skaugen, Knut Alfredsen and Tone M. Muthanna

ABSTRACT

Floods are one of the major climate-related hazards and cause casualties and substantial damage. Accurate and timely flood forecasting and design flood estimation are important to protect lives and property. The Distance Distribution Dynamic (DDD) is a parsimonious rainfall-runoff model which is being used for flood forecasting at the Norwegian flood forecasting service. The model, like many other models, underestimates floods in many cases. To improve the flood peak prediction, we propose a dynamic river network method into the model. The method is applied for 15 catchments in Norway and tested on 91 flood peaks. The performance of DDD in terms of KGE and BIAS is identical with and without dynamic river network, but the relative error (RE) and mean absolute relative error (MARE) of the simulated flood peaks are improved significantly with the method. The 0.75 and 0.25 quantiles of the RE are reduced from 41% to 23% and from 22% to 1%, respectively. The MARE is reduced from 32.9% to 15.7%. The study results also show that the critical support area is smaller in steep and bare mountain catchments than flat and forested catchments.

Key words | critical flux (FC), critical supporting area (AC), dynamic river network, floods

Aynalem Tassachew Tsegaw (corresponding author)
Knut Alfredsen
Tone M. Muthanna
Civil and Environmental Engineering,
Norwegian University of Science and Technology,
SP Andersen Vei 5, Trondheim 7491,
Norway
E-mail: *aynalem.t.tasachew@ntnu.no*

Thomas Skaugen
Hydrology Department,
Norwegian Water Resources and Energy Directorate (NVE),
PO Box 5091, Oslo 0301,
Norway

INTRODUCTION

Floods are one of the major climate-related hazards and cause casualties and substantial damage on a global scale every year (Hirabayashi *et al.* 2013; Blaikie *et al.* 2014; Winsemius *et al.* 2015). Floods usually cause damage to agricultural land, infrastructure and buildings (Razi *et al.* 2010). Flood peak is one of the most important variables to be estimated as its magnitude and duration are responsible for the damage (Formetta *et al.* 2017; Gao *et al.* 2017). An accurate estimate of flood peak is a critical requirement for proposing appropriate flood damage mitigation measures in order to reduce social and economic costs (Plate 2009).

The common hydrological tools for flood risk management are flood forecasting models and models used to estimate design floods (Plate 2009). The design flood, where the magnitude of the flood is associated with a return period and hence a level of risk, is important in the planning, design and operation of hydraulic structures and for protection of human life and property (Rahman *et al.* 1998; Reis & Stedinger 2005; Smithers 2012). Methods to estimate design floods are generally classified into three: (a) statistical flood frequency analysis; (b) event-based simulation; and (c) derived flood frequency simulation (Filipova *et al.* 2018).

Derived flood frequency analysis, using continuous rainfall-runoff models, is increasing in use for design flood

doi: 10.2166/nh.2019.003

estimation (Cameron *et al.* 2000; Calver & Lamb 1995; Boughton & Droop 2003; Eschenbach *et al.* 2008). A rainfall-runoff model can be used to simulate several flow values under different conditions for extending and enhancing the observed flow record (Filipova *et al.* 2018). A stochastic weather generator is used to simulate long synthetic series of rainfall and temperature input data for the continuous simulation method. The long series of flow data derived from the simulation is then used to estimate the required return periods, usually using plotting positions (Camici *et al.* 2011; Haberlandt & Radtke 2014). There is a growing interest in continuous simulation method of flood estimation as an alternative to event-based method, and internationally the trend is to adopt the continuous method (Lamb & Kay 2004; Chetty & Smithers 2005; Pathiraja *et al.* 2012). The main advantages of the continuous simulation models are their ability to represent the antecedent moisture condition in the catchment and their capability to model future land use and climate changes impacts on the flood peaks (Brocca *et al.* 2011; Smithers *et al.* 2013). The other reason for using the continuous simulation approach is that precipitation records are more widely available and tend to have longer periods of records than stream flow data (Blazkova & Beven 2002). Continuous simulation can avoid the base flow estimation problem in the event-based method and avoid any need to associate return period of the flood with specific design precipitation because the frequency analysis of floods can be done directly.

Rainfall-runoff models are simplified representations of a complex physical system and therefore carry a certain amount of uncertainty in their applications (Bourdin *et al.* 2012). The performance of rainfall-runoff models depend on several factors which include the quality of precipitation input data and an appropriate model structure capable of simulating floods (Collier 2007). Therefore, the structure and performance of the rainfall-runoff models should be evaluated and improved for their capability in simulating flood peaks before using them in design flood estimation and flood forecasting.

There are several ways to classify rainfall-runoff models (Singh 1995). Rainfall-runoff models can be classified into lumped and distributed models. Lumped models consider the whole catchment as a single unit with state variables that represent the average of the catchment (Beven 2001b). Distributed models make prediction at distributed locations, i.e., by discretizing the catchment into a number of elements with state variables representing local averages (Singh & Frevert 2006). When a rainfall-runoff model is used for design flood estimation, the model could underestimate the design flood. Thomas (1982) evaluated floods estimated by continuous simulation methods on 50 small streams in Oklahoma, and the result showed that the flood peaks were consistently underestimated. Pathiraja *et al.* (2012) used 45 catchments in the Murray–Darling basin in Australia to estimate design floods using the Australian water balance model. They found that the model underestimates the floods from 5% to 30% depending on how reasonably the antecedent moisture condition is simulated. The forecast of floods requires an accurate understanding of catchment characteristics and a precise determination of catchment's initial conditions before flooding (Rusjan *et al.* 2009).

There is a link between catchment morphology and a hydrologic response of a catchment (Rodríguez-Iturbe & Valdés 1979; D'Odorico & Rigon 2003; Rigon *et al.* 2011). Gupta *et al.* (1980) pointed out that the Geomorphic Instantaneous Unit Hydrograph (GIUH) is equivalent to the probability density function of travel times, $f(t)$, from any point in the catchment to the outlet. This permits the formulation of hydrologic response through the geomorphologic width function, $W(x)$. The GIUH and $W(x)$ concepts represent the dependency of peak flows on the geomorphological properties of a catchment and provide a quantitative prediction of peak flows for engineering application (Rinaldo *et al.* 1991; Rinaldo *et al.* 1995; D'Odorico & Rigon 2003; Rigon *et al.* 2011). The form and extent of the stream network reflect the characteristics of the hillslope (Willgoose *et al.* 1991). The stream reflects the ground water dynamics and is often termed as perennial, intermittent and ephemeral streams (Dingman 1978; Bencala *et al.* 2011). Dynamic expansions and contractions of stream networks play an important role for hydrologic processes since they connect different parts of the catchment to the outlet (Nhim 2012). Stream networks in a catchment expand and contract as the catchment wets and dries, both seasonally and in response to individual precipitation events, and this dynamic of stream networks gives an

important information to the pattern and process of runoff generation (Godsey & Kirchner 2014; Ward *et al.* 2018). The mean of the distribution of distances from a point in the catchment to the nearest river reach (D_m) and the drainage density (D_d) are among the indexes used to describe a stream network. Horton (1945) defined the traditional D_d as the sum of lengths (L) of all streams in a catchment divided by the catchment area (A). The D_m reflects the spatial characteristics that affect the formation of streams and the response time of a catchment for a particular stream network (Wharton 1994; Tucker *et al.* 2001; Di Lazzaro *et al.* 2014; Skaugen & Onof 2014). The mean distance one has to walk from a random location in a hillslope before encountering a stream, D_m is related to the traditional definition of D_d (Horton 1932; Tucker *et al.* 2001; Di Lazzaro *et al.* 2014).

$$D_m \approx \frac{1}{2D_d} \tag{1}$$

Chorley & Morgan (1962) showed that the maximum flow is related to D_m. Day (1983) studied two catchments of New England (NSW, Australia) and found that the D_m is correlated with discharge. In these two catchments, the D_m was found to decrease for an increase in discharge, indicating that the stream network expands during the flooding events. During the expansion and contraction of streams, the critical supporting area (A_c), which is the area needed to initiate and maintain streams, shows variations within a catchment and is an important variable for assessing geomorphometric characteristics (e.g. D_m) (Papageorgaki & Nalbantis 2017). The relationship between D_d and A_c follows an inverse power law (Moglen *et al.* 1998) as shown in Equation (2):

$$D_d = kA_c^{-n} \tag{2}$$

where k and n are positive numbers. If we insert the value of D_d from Equation (2) into Equation (1), we will get a power relationship between D_m and A_c as shown in Equation (3):

$$D_m = aA_c^b \tag{3}$$

where $a = 1/2k$ and $b = n$.

The Distance Distributions Dynamics (DDD) model is a parsimonious continuous rainfall-runoff model with a small number of calibration parameters recently developed by Skaugen & Onof (2014). Many of the model parameters can be estimated from catchment topography using geographic information system (GIS) and recession characteristics. DDD is a semi-distributed model, i.e., lumped in model parameters and distributed input data (precipitation and temperature). The calibration and validation results for 41 small rural unregulated catchments in Norway (area <50 km^2) with hourly data showed that the DDD model, in most cases, underestimated flood peaks (Tsegaw *et al.* 2019). In the runoff dynamics of the DDD model, there is a single static river network forming the basis for the dynamics of water routing through the hillslopes and in the river network (Skaugen & Onof 2014). However, studies show that the river network has a dynamical nature, being more dense during high flows than at low or medium flows (Godsey & Kirchner 2014). The primary objective of this study is to investigate whether including a dynamic river network model into the DDD model will improve flood prediction in small rural catchments (area <50 km^2). The secondary objective is to improve the understanding of the stream development for different vegetation covers, catchment slopes and climate. The secondary objective helps us to assess whether there is a potential to relate a calibration parameter of the dynamic river network routine with the environmental factors so that there is a possibility for regionalizing the parameter.

METHODOLOGY

Study catchments and data

Fifteen gauged small rural catchments, which show significant underestimation of peak floods during the calibration and validation of 41 small catchments located in Norway (Tsegaw *et al.* 2019), are used in this study for testing the dynamic river network method. The catchments are selected from the Norwegian Water Resources and Energy Directorate (NVE) HYDRA II database. Figure 1 shows locations of the study catchments, and Table 1 shows the catchment characteristics. The definition of small catchment follows that of Fleig & Wilson (2013) with an upper area limit of

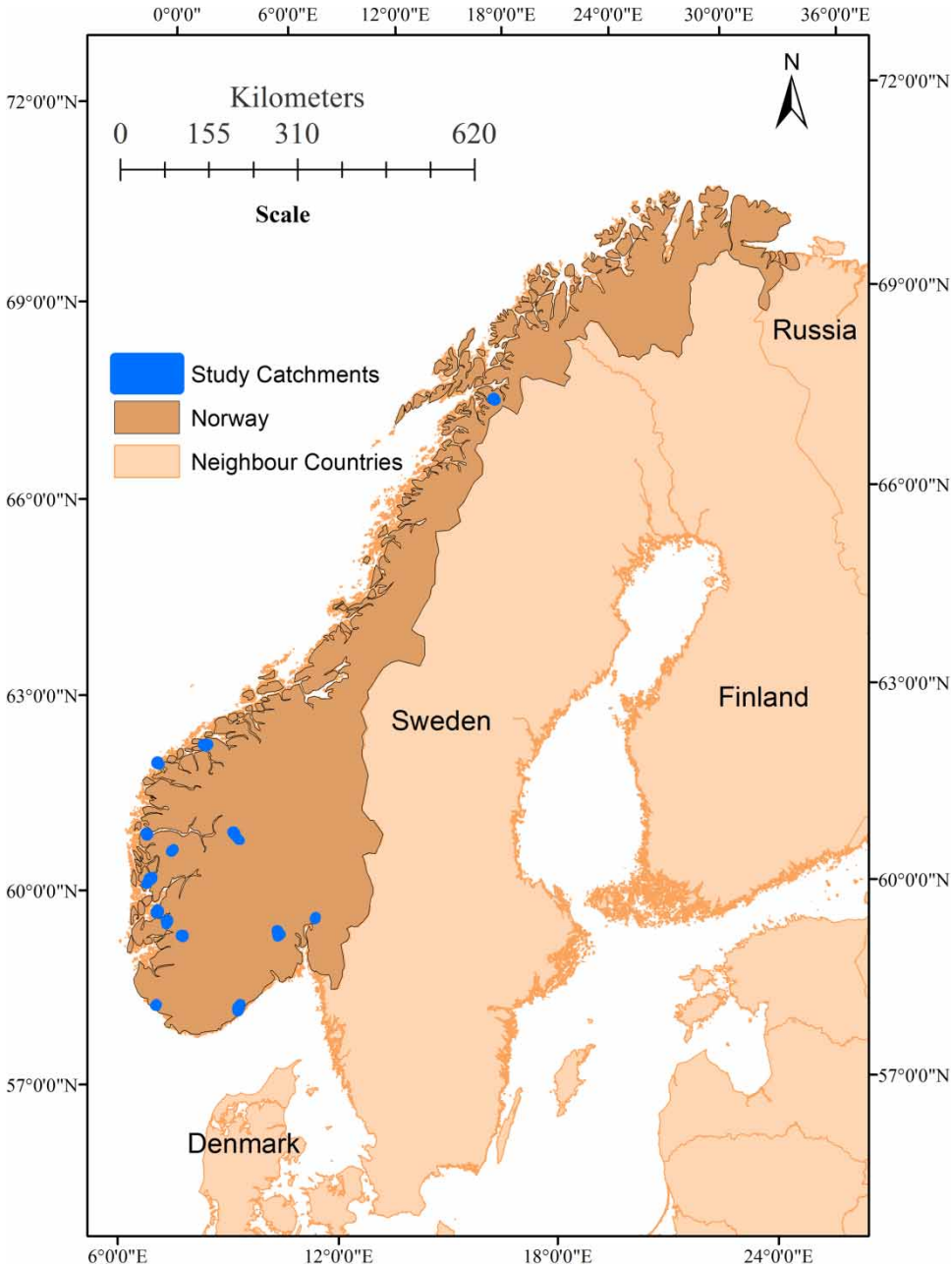

Figure 1 | Locations of study catchments.

50 km^2. We selected where the DDD model had a known history of underestimating floods so that the dynamic river network model could be tested and evaluated.

Precipitation, temperature and discharge are the main input data for running and calibrating the DDD model. We used hourly data of precipitation, temperature and discharge. Precipitation and temperature are based on a 1×1 km gridded product of the Norwegian Meteorological Institute (http://thredds.met.no/thredds/catalog.html) (Lussana *et al.* 2016). We used a total of 5 years of data for calibration and validation. The DDD model uses distributed precipitation and temperature data as input for the model's 10 elevation zones extracted from the hypsographic curve of a catchment. The elevation of the center of each

Table 1 | Catchment characteristics of the study catchments

S.no	Cat_ID	Area (km^2)	Lake (%)	Marsh land (%)	Forest (%)	Bare mountain (%)	Cultivated land (%)	Urban (%)	Mean elvation (m)	Mean annual precipitation (mm)	Mean annual temprature (°C)	Specific runoff ($l/s/km^2$)	Mean hillslope slope (%)
1	6.10	7	2.7	1.6	94.3	0	0	0	302.9	886	4.1	20.6	18.3
2	12.193	50.7	1.3	3	88.4	0	4.3	0.5	306.5	840	3.8	17.5	15.3
3	19.107	41.5	4.8	1.4	86.4	0	4.2	0.8	88.4	1,158	4.2	24.2	14.7
4	26.64	9.7	7.2	2.2	38.8	46.2	1.1	0	203.9	1,688	6.7	45.8	28.3
5	36.32	20.9	2.5	0.9	13.5	81.4	0	0	1,039.4	2,377	0.2	105.2	34.1
6	41.8	27.4	7.7	0.4	8.8	82.2	0	0	836.8	2,955	2.7	126.4	37.5
7	42.2	31.1	2.8	1.4	40.7	52.1	0	0	573.3	2,361	4.8	108.3	40.4
8	55.4	50.6	3.7	1.3	51.8	30.7	2.8	0.2	361.3	2,593	5.4	100.4	41.9
9	63.12	12.8	4.5	0.3	5.8	86.1	0.6	0	886.2	2,579	1.1	94.8	34.4
10	68.2	20.9	4.3	0	20.2	50.3	2.5	0	402.4	2,736	5	125.2	43.6
11	73.21	25.8	7.4	2.2	2.2	88	0	0	1,292.5	946	−0.8	34.7	21.5
12	73.27	30.4	9.1	0.5	0.1	89.4	0	0	1,372	679	−2.5	33.5	14.8
13	91.2	25.8	10.1	3	3.7	66.5	1.3	0	261.9	2,072	6.1	63.5	29.9
14	101.1	40	11.3	1.6	61.3	11.3	6	0.1	232.9	1,704	5.5	54.9	23.9
15	172.8	21.2	10.7	0.5	1.4	82.5	0	0	659	1,465	1	46	17
Minimum		7	1.3	0	0.1	0	0	0	88.4	679	−2.5	17.5	14.7
Maximum		50.7	11.3	3	94.3	89.4	6	0.8	1,372	2,955	6.7	126.4	43.6

temperature and precipitation grid cell has been extracted from the 10×10 m digital elevation model (DEM) of Norway. Discharge data have been obtained from the Norwegian Water Resources and Energy Directorates (NVE) HYDRA II database. The Norwegian Mapping Authority (www.statkart.no) is the source of the topography, observed river network and land use data.

The DDD rainfall-runoff model

The DDD model currently runs operationally with daily and three-hourly time steps at the Norwegian flood forecasting service. It has two main modules: the subsurface and the dynamics of runoff. In DDD, the distribution of distances between points in the catchment and their nearest river reach (distance distributions of a hillslope) is the basis for describing the flow dynamics of the hillslope. The distribution of distances between points in the river network and the outlet forms the basis for describing the flow dynamics of the river network. The hillslope and river flow dynamics of DDD is hence described by unit hydrographs (UHs) derived from distance distributions from a GIS and celerity derived from recession analysis (Skaugen & Onof 2014; Skaugen & Mengistu 2016). When the distance distributions are associated with flow celerity of the hillslope and rivers, we obtain the distributions of travel times which constitute the time area concentration curve (Maidment 1993). The derivative of the time area concentration curve gives the instantaneous UH (Bras 1990), which is basically a set of weights distributing the input (precipitation and snowmelt) in time to the outlet.

Subsurface

The volume capacity of the subsurface water reservoir, M (mm), is shared between a saturated zone with volume S (mm) and an unsaturated zone with volume D (mm). If the volume of the saturated zone is high, the unsaturated volume has to be correspondingly small (Skaugen & Onof 2014; Skaugen & Mengistu 2016). The actual water volume present in the unsaturated zone is described as Z (mm). The subsurface state variables are updated after evaluating whether the current soil moisture, $Z(t)$, together with the input of rain and snowmelt, $G(t)$, represent an excess of water over the field capacity, R, which is fixed at 30% ($R = 0.3$) of $D(t)$ (Skaugen & Onof 2014). If $G(t) + Z(t) > R^*D(t)$, then the excess water $X(t)$ is added to $S(t)$.

Excess water (mm/h)

$$X(t) = \text{Max}\left\{\frac{G(t) + Z(t)}{D(t)} - R,\ 0\right\} D(t) \tag{4}$$

Ground water (mm/h) $$\frac{dS}{dt} = X(t) - Q(t) \tag{5}$$

Soil water content (mm/h) $$\frac{d\,Z}{dt} = G(t) - X(t) - E_a(t) \tag{6}$$

Soil water zone (mm/h) $$\frac{dD}{dt} = -\frac{dS}{dt} \tag{7}$$

Potential evapotranspiration (mm/h) $$E_p = Cea * T \tag{8}$$

Actual evapotranspiration (mm/h) $$E_a = E_p * \frac{S + Z}{M} \tag{9}$$

$Q(t)$ is runoff, and $E_a(t)$ is the actual evapotranspiration which is estimated as a function of potential evapotranspiration and the level of storage. Cea is a degree hour factor which is positive for positive temperature (T) and zero for negative temperature. E_a is drawn from Z. The degree hour approach is a simplification but experiences from Skaugen & Onof (2014) show that the evapotranspiration routine in DDD calculates similar values to the approach used in the well-known rainfall-runoff model HBV (Bergström 1976). A recession analysis of observed runoff from the catchment is used to estimate the catchment-scale fluctuations of storage and the capacity of the subsurface water reservoir (M) (see Skaugen & Mengistu 2016).

Runoff dynamics

The dynamics of runoff in DDD has been derived from the catchment features using a GIS combined with runoff recession analysis. The method for describing the runoff dynamics of a catchment is built on the distance distribution derived from the catchment topography. The distances from the points in the catchment to the nearest river reach are calculated as Euclidean distance for the marsh and soil parts of a hillslope. Previous studies in more than 120 catchments in

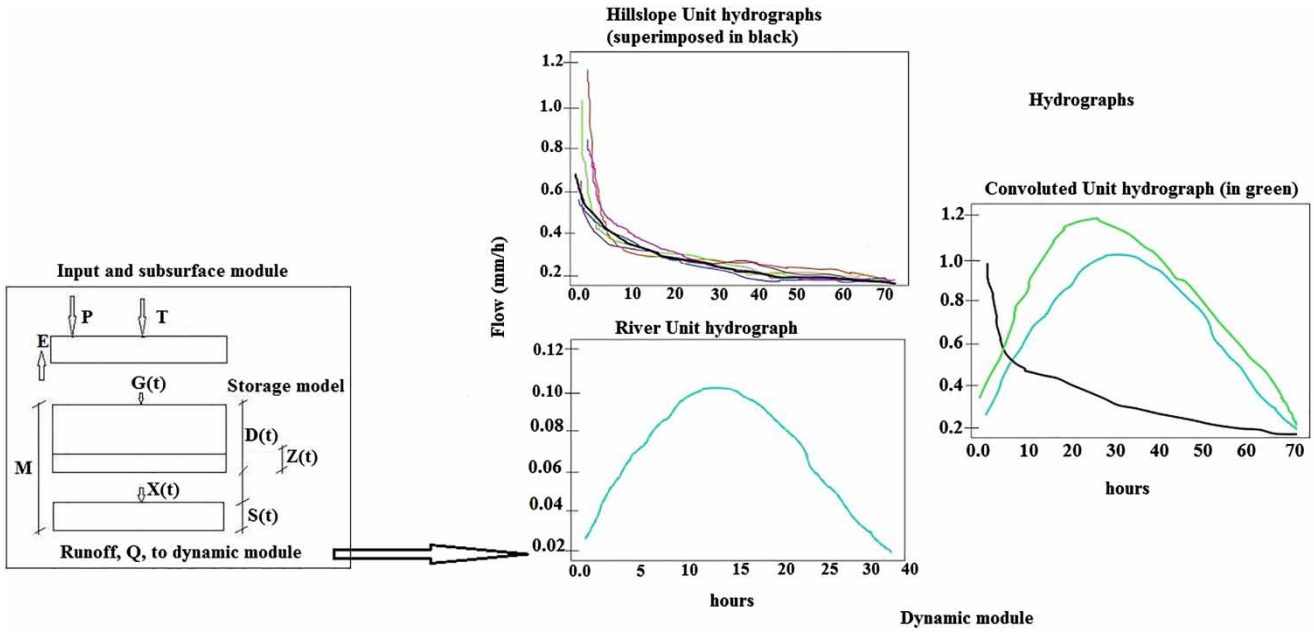

Figure 2 | Structure of distance distribution dynamics (DDD) rainfall-runoff model. Please refer to the online version of this paper to see this figure in colour: http://dx.doi.org/10.2166/nh.2019.003.

Norway showed that the exponential distribution describes the hillslope distance (Euclidean distance from the nearest river reach) distribution well, and the normal distribution describes well the distances between points in the river network and outlet of a catchment (Skaugen & Onof 2014). Figure 2 shows the structure of the DDD model. The model is written in the R programming language. All GIS work is done with ArcGIS 10.3 (ESRI 2014), and the recession analysis is done using an R script (R Core Team 2017).

Water is conveyed through the soils to the river network by waves with celerity determined by the actual storage, $S(t)$, in the catchment (Skaugen & Onof 2014; Skaugen & Mengistu 2016). The celerity associated with the different levels of subsurface storage is estimated by assuming exponential recessions with parameter Λ in the equation $Q(t) = Q_0 \Lambda e^{-\Lambda(t-t_0)}$, where Q_0 is the peak discharge immediately before the recession starts. Λ is the slope per Δt of the recession in the log–log space.

$$\Lambda(t) = \log(Q(t)) - log(Q(t+\Delta t)) \tag{10}$$

The distribution of Λ is modeled using a two-parameter gamma distribution.

The celerity, v, is calculated as a function of Λ using Equation (11):

$$v = \frac{\Lambda \ D_{\mathrm{m}}}{\Delta t} \tag{11}$$

where, D_{m} is the mean of the distances from points in the catchment (hillslope) to the nearest river. The capacity of the subsurface reservoir M (mm) is divided into five storage levels, i, corresponding to the quantiles of the distribution of Λ under the assumption that the higher the storage, the higher the value of Λ. Each storage level is further assigned a celerity $v_i = \frac{\lambda_i \ D_{\mathrm{m}}}{\Delta t}$ (see Equation (11)), where λ_i is the parameter of the UH for the individual storage level i, and estimated such that the runoff from several storage levels will give a UH equal to the exponential UH with a parameter Λ_i. With the assumption that the recession and its distribution carries information on the distribution of catchment-scale storage, we can consider that the temporal distribution of catchment-scale storage, $S(t)$, is a scaled version to that of Λ. $S(t)$ is calculated using Equation (12), and its distribution is modeled using a two-parameter gamma distribution.

$$S(t) = \frac{Q(t)}{1 - \ e^{-\Lambda(t)}} \tag{12}$$

The DDD model has five storage levels ($i = 1, \ldots, 5$). Four storage levels are subsurface level, whereas the fifth one is an overland flow level with unlimited capacity (Skaugen & Onof 2014; Skaugen & Mengistu 2016). The five levels have five-UHs (four for subsurface flow and one for overland flow) and each of them has different temporal scales as they have been assigned different celerities. The UH is modeled as follows:

$$\mathrm{UH}_i(t) = \lambda_i \mathrm{e}^{-\lambda_i(t-t_\mathrm{o})} \tag{13}$$

where t_o is the time of input, and λ_i is the parameter of the exponential distribution estimated from recession analysis for each level, i.

Model parameters and calibration

The model parameters are divided into three main groups. The first group are those estimated from observed hydro-meteorological data (Table 2), the second group are those estimated by model calibration against observed discharge (Table 3), and the third group are those estimated from digitized maps using a GIS (Table 4). The snow routine in DDD has two parameters estimated from the spatial distribution of observed precipitation data (Skaugen & Weltzien 2016). The shape parameter (a_0) and the decorrelation length (d) of the gamma distribution of snow and snow water equivalent (SWE) are estimated from a previous calibration for 84 catchments in Norway (Skaugen *et al.* 2015). The calibration of the model is performed using the probability particle swarm optimization (PPSO) algorithm (Lu & Han 2011). The Kling–Gupta efficiency criteria (KGE) have been used as objective function for the calibration (Gupta *et al.* 2009), and we used KGE, the BIAS (ratio of the mean of simulated to observed discharge) and visual inspection of hydrographs to evaluate the performance of the model.

Dynamic river network routine

We introduce a dynamic river network concept into the DDD model so that the scale of the overland unit hydrograph (OUH) will be dynamic while keeping the four

Table 2 | List of DDD rainfall-runoff model parameters estimated from observed hydro-meteorological data

Parameters	Description of the parameter	Method of estimation	Unit
d	Parameter for spatial distribution of SWE, decorrelation length	From spatial distribution of observed precipitation	Positive real number
a0	Parameter for spatial distribution of SWE, shape parameter	From spatial distribution of observed precipitation	Positive real number
MAD	Long-term mean annual discharge	From long-term observed mean annual flow data	m^3/s
Gshape	Shape parameter of λ	Recession analysis of observed runoff	Positive real number
Gscale	Scale parameter of λ	Recession analysis of observed runoff	Positive real number
GshInt	Shape parameter of Λ	Recession analysis of observed runoff	Positive real number
GscInt	Scale parameter of Λ	Recession analysis of observed runoff	Positive real number

Table 3 | List of DDD rainfall-runoff model parameters needing calibration

Parameters	Description of the parameter	Method of estimation	Unit	Intervals of calibration
pro	Liquid water in snow	Calibration	fraction	0.03–0.1
cx	Degree hour factor for snow melt	Calibration	$mm\,^\circ C^{-1}\,h^{-1}$	0.05–1.0
CFR	Degree hour factor for refreezing	Calibration	$mm\,^\circ C^{-1}\,h^{-1}$	0.001–0.01
Cea	Degree hour factor for evapotranspiration	Calibration	$mm\,^\circ C^{-1}\,h^{-1}$	0.01–0.1
rv	Celerity for river flow	Calibration	m/s	0.5–1.5

Table 4 | List of DDD rainfall-runoff model parameters estimated from geographical data using GIS

Symbol of parameters	Description of the parameter
Area	Catchment area
maxLbog	Maximum distance of marsh land portion of hillslope
midLbog	Mean distance of marsh land portion of hillslope
bogfrac	Areal fraction of marsh land from the total land uses
zsoil	Areal fraction of DD for soils (what area with distance zero to the river)
zbog	Areal fraction of distance distribution for marsh land (what area with distance zero to the river)
midFl	Mean distance (from distance distribution) for river network
stdFL	Standard deviation of distance (from distance distribution) for river network
maxFL	Maximum distance (from distance distribution) for river network
maxDl	Maximum distance (from distance distribution) of non-marsh land (soils) of hill slope
midDL	Mean distance (from distance distribution) of non-marsh land (soils) of hill slope
midGl	Mean distance (from distance distribution) for glaciers
stdGl	Standard deviation of distance (from distance distribution) for glaciers
maxGl	Maximum distance (from distance distribution) for glaciers
Hypsographic curve	11 values describing the quantiles 0, 10, 20, 30, 40, 50, 60, 70, 80, 90, 100

subsurface UHs constant during the simulation period. The methodology, we used in estimating the dynamic OUHs of a hillslope, is similar to that of GIUH and of the width function, i.e., the travel time probability density function of a unit amount of water draining from a catchment. However, the approaches used in estimating the parameters of the distribution are different, i.e., the approach in calculating the celerity and distances of a flow from the points in the hillslope to the nearest river reach. Further, we assumed that the scale of the travel time distribution in a hillslope is dynamic for generating dynamic OUHs while the shape is held constant. In DDD, the dynamic OUHs are turned on and off according to saturation of the subsurface thus giving a dynamic travel time distribution.

The river network indicates where the subsurface water flow becomes surface water flow. The network system governs the dynamics of runoff for conditions where we have no overland flow from the hillslope in that there is a significant (orders of magnitude) difference in water celerity for flow through the soils and flow in the river network (Robinson *et al.* 1995). In case of overland flow, however, we can imagine a dynamic river network (and hence dynamic distance distributions) as a function of overland flow (OF). We made three assumptions to derive such algorithm.

1. The mean celerity of the overland flow (v_{OF}) is constant, i.e., independent of the subsurface saturation and river network.
2. The overland flow unit hydrograph (OUH) is exponential determined from D_m and v_{OF}.
3. The D_m of a river network is a function of volume of water per area per unit time, i.e., OF. If we assume a critical flux, F_c of 10 m^3/h is necessary to create a stream, then OF of 10 mm for an hour over $A_c = 1000\ m^2$, will provide such a flux, whereas the same flux is obtained for OF of 100 mm over 100 m^2. The two cases have different critical supporting area (A_c), and these cases will provide us with two different river networks where the latter has smaller D_m than the former.

The physical mechanisms underpinning the above three assumptions are:

1. The variable contributions of saturation excess overland flow of a hillslope develops along the existing river network following the concept of Dunne's overland flow (Dunne 1978).
2. The critical supporting area (A_c defines the minimum catchment area from which the generated runoff is sufficient to initiate and maintain river development

(Schaefer *et al.* 1979)). The expansion and contraction of the stream network is governed by the amount of saturation excess overland flow.

3. The hillslope travel time probability density function of overland flow is estimated from the distance distributions at any point from the hillslope to the river network and the celerity of flow in the hillslope (D'Odorico & Rigon 2003; Rigon *et al.* 2011).

In order to compute the OUH, we need the mean (D_m) and the maximum (D_{max}) of the hillslope distance distribution and the mean overland flow celerity, v_{OF}. Using assumption (3), we can derive a dynamic A_c after introducing a critical flux (F_c) as shown in Equation (14), which needs to be determined.

$$F_c\,(m^3/h) = A_c(\mathrm{m}^2) * \mathrm{OF}\ (\mathrm{m/h}) \tag{14}$$

where OF is saturation excess overland flow and is estimated from the DDD model output at each simulation time step. When the subsurface is saturated and there is overland flow (OF > 0), the dynamic river network subroutine is activated and the corresponding A_c will be calculated in the model using Equation (14).

We need to compute the coefficients a and b of the general power relation between D_m and A_c of each of the study catchments (see Equation (3)) for computing a dynamic D_m during simulation. For computing a and b, we have used the following procedure:

1. The 10×10 m DEM of a catchment has been reconditioned to the observed river network using the DEM reconditioning tool from Arc Hydro and a raster flow accumulation map has been prepared using GIS.
2. We wrote a python script that can loop through several thresholds of flow accumulation (A_c) to define stream and create several stream networks. From the distance distributions derived from each stream networks, the D_m is calculated.
3. A regression curve is fitted to the synthetically derived A_c and D_m of a catchment to estimate a and b (Figure 3 shows the fitted curves for six sample catchments). The values of a and b are unique for each catchment and are listed in Table 5 for all study catchments.

After we have obtained the coefficients of the relationship between A_c and D_m, the A_c estimated from Equation (14) will be used to estimate D_m using Equation (3). We estimated D_{mx} from the exponential distribution with parameter D_m, as a distance where 99% of the catchment area is accounted for. From the recession analysis for estimating celerities, we already have an estimate of v_{OF} in the DDD model (Skaugen & Onof 2014). We estimate a dynamic OUH for every time step when overland flow is estimated.

When the D_m calculated using Equation (3) is greater than the D_m of the observed river network, the dynamic river network degenerates to the observed river network. The observed river network is the basis network for all cases where the subsurface capacity is unsaturated, saturated but no overland flow and when there is overland flow but not sufficient to expand the observed (existing) stream network. When the subsurface capacity is saturated and there is sufficient OF, the observed stream network starts to expand. The extent of expansion is determined by the magnitude of the estimated OF and F_c.

We have tested the performance of the DDD model with and without the dynamic river network routine. We calibrated and validated the DDD model as described in the model parameter and calibration section, and we implemented the dynamic river routine into the model and calibrated F_c. We have calibrated F_c manually after calibrating automatically DDD parameters without dynamic river network. The procedures we have followed in calibrating are as follows:

1. The F_c parameter is adjusted by trial and error to fit the observed flood peaks, which had been underestimated by DDD without dynamic river network.
2. We have visually compared the observed flood hydrographs and flood hydrographs simulated with and without dynamic river network.
3. While calibrating DDD with F_c (with dynamic river network module), the KGE and BIAS values obtained should not be less than the KGE and BIAS values of DDD without dynamic river network method (earlier calibration result).
4. Using the visual inspection of observed hydrographs, KGE and BIAS, the F_c which fits the observed flood peaks well is taken as a calibrated value.

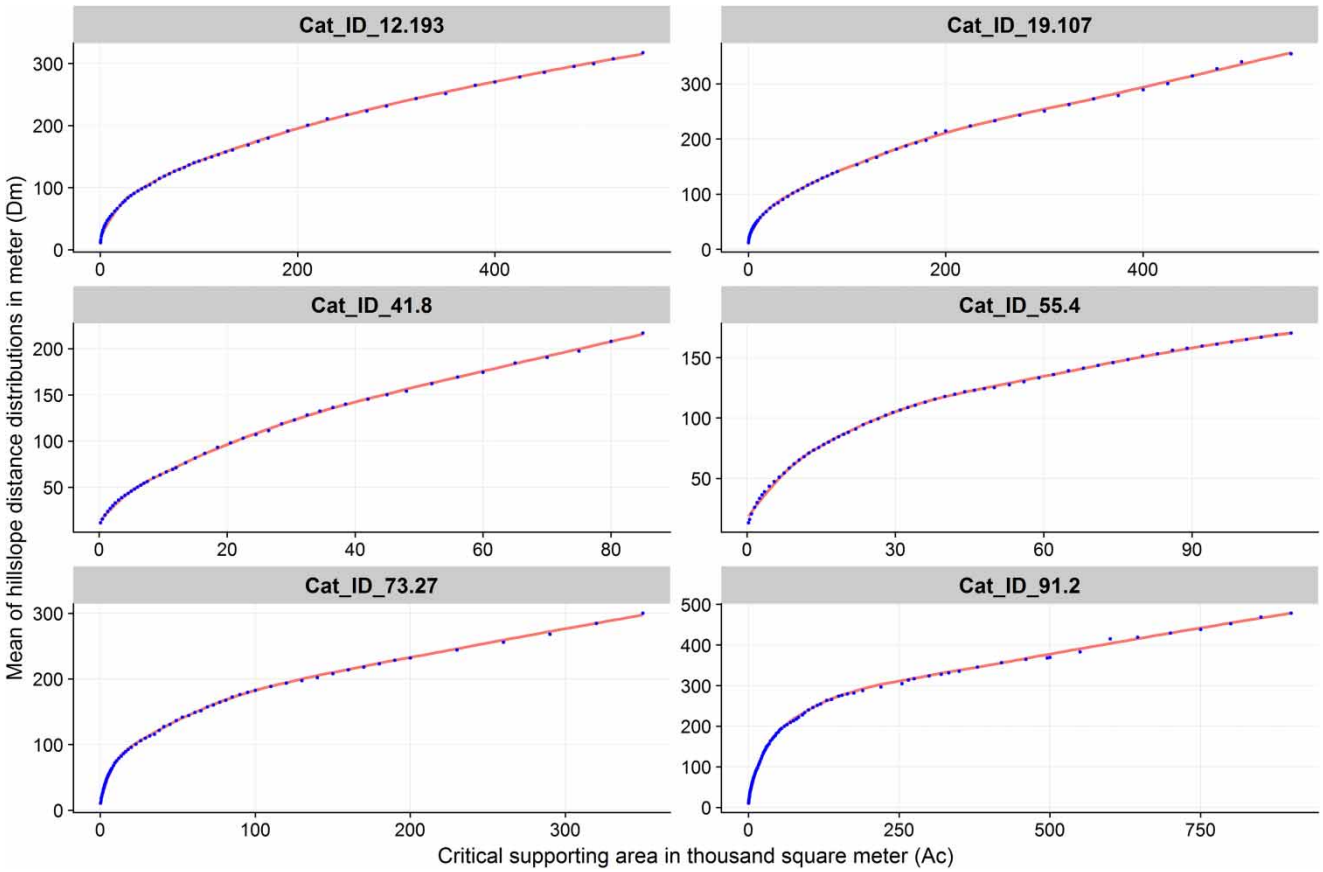

Figure 3 | Curves fitted to the relation between mean distance distribution of hillslope, i.e., D_m and critical supporting area, i.e., A_c for six sample study catchments with a relation, $D_m = aA_c^b$.

As for the previous case, we used KGE, BIAS and hydrographs to evaluate the performance of the model with dynamic river network routine. We have also analyzed the mean absolute relative error (MARE, Equation (15)) of 91 flood peaks with and without river dynamics.

$$\text{MARE}(\%) = \frac{1}{N}\sum_{i=1}^{N}\left|\frac{(O_i - S_i)}{O_i} * 100\right| \quad (15)$$

where O_i is the observed flood peak and S_i is the predicted flood peak with and without dynamic river network. N is the number of flood peaks (91 in this study). We have also analyzed the quantiles of the distribution of relative errors (RE, Equation (16)) of the flood peaks prediction.

$$\text{RE}(\%) = \frac{(O_i - S_i)}{O_i} * 100 \quad (16)$$

where O_i is the observed flood peak and S_i is the predicted flood peak with and without dynamic river network.

Correlation between A_c and F_c with environmental factors

We have done a correlation analysis between the parameters A_c and F_c and environmental factors to improve the understanding on how the dynamic river network develops and to assess the potential for relating F_c to environmental factors. The environmental factors included in the correlation analysis are mean annual precipitation, mean hillslope slope, bare mountain and forest land covers of the study catchments. We have used the Pearson correlation coefficient for the analysis. The A_c derived from observed river network has a spatial variation within a catchment; therefore, we have estimated the mean A_c for

Table 5 | The coefficient of determination (R-squared) and the coefficients of the power relation between D_m and A_c, i.e., $D_m = aA_c^b$ for all the study catchments

Cat_ID	a	b	R^2
6.1	2.17	0.37	0.99
12.193	1.16	0.42	1
19.107	1.04	0.43	1
26.64	1.23	0.42	1
36.32	1.18	0.42	1
41.8	0.61	0.51	0.99
42.2	0.92	0.45	1
55.4	1.1	0.44	1
63.12	1.05	0.45	1
68.2	0.86	0.49	1
73.21	0.82	0.48	1
73.27	1.19	0.44	0.99
91.2	0.68	0.51	0.99
101.1	1.1	0.45	0.98
172.8	1.08	0.44	1

each of the study catchments before the correlation analysis using the following two steps. First, the D_m of the observed stream network is estimated using GIS. Second, the mean A_c of the observed river network is calculated using Equation (3). To assess the potential for relating F_c with the environmental factors, correlation analysis between the calibrated F_c and the environmental factors has also been performed. We have also done a stepwise method of multiple linear regression between F_c and the four environmental factors mentioned above to see if there is a possibility for regionalizing F_c.

RESULTS

Performance of DDD with and without dynamic river network

The calibration and validation results of the DDD model without a dynamic river network show that the model performs satisfactorily with KGE values between 0.55 and 0.9 and BIAS between 0.75 and 1.25. As stated by Thiemig *et al.* (2013), $0.75 \leq \text{KGE} < 0.9$ is considered good, $0.5 \leq \text{KGE} < 0.75$ is intermediate and $0.0 \leq \text{KGE} < 0.5$ is poor. Seven catchments show good and eight catchments show intermediate performance both during the calibration and validation periods. Even if the KGE performance is satisfactory, the visual inspection of the hydrographs shows that several observed flood peaks are underestimated.

We added the dynamic river network routine into the DDD model and calibrated the critical flux (F_c) parameter of the routine manually for the whole simulation period. The KGE and BIAS performance of the model are similar as before, i.e., without dynamic river network for all study catchments except one, where the KGE is slightly lower. However, the inspection of the hydrographs clearly shows that the predication of several underestimated flood peaks has been improved after the addition of the dynamic river network routine. The dynamic OUHs that resulted from the dynamic river network have higher peaks and narrower width during the flooding events, and these OUHs, added with the subsurface UHs, helped in improving the previously underestimated floods. Figure 4 shows the hillslope distance distributions for variable A_c for catchment 73.27. Figure 5 shows the empirical cumulative distance distributions functions as an example for the dynamic distance distribution presented in Figure 4, and Figure 6 shows the four dynamic OUHs which resulted from the corresponding distance distributions functions. Table 6 shows OF, A_c and D_m for a catchment 12.193 during a flooding event.

Figure 7 shows the hydrographs during the flooding periods with and without the dynamic river network routine for six sample study catchments. Table 7 shows the observed floods, simulated floods, KGE and BIAS performance of DDD model with and without dynamic river network routine for five sample study catchments selected randomly.

The results of the statistical analysis (mean absolute relative errors and quantiles of relative errors), for the 91 observed peak floods from the 15 study catchments, show that the dynamic river network method improved the prediction of peak floods significantly. The 0.75 quantile of the relative errors of the simulated peaks reduced from 41% to 23%, and the 0.25 quantile of the relative errors reduced from 22% to 1%. Figure 8 shows box plots of the relative errors with and without river dynamics. The MARE of the magnitude of the underestimated peak floods is reduced from 32.9% to 15.7%.

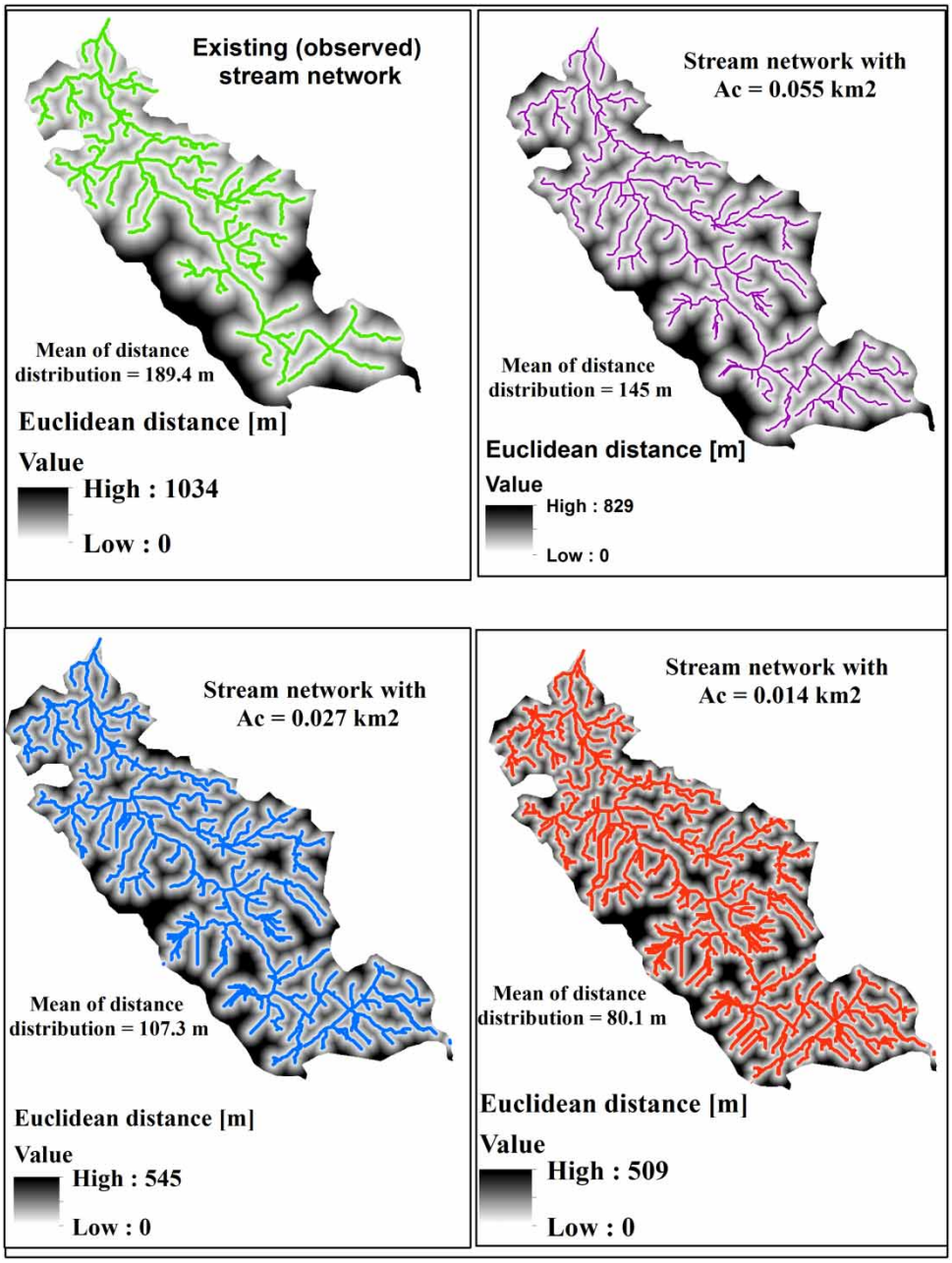

Figure 4 | Map of sample dynamic distance distributions of hillslope generated from dynamic critical supporting area, i.e., A_c during flooding events for catchment 73.27.

Correlation between A_c and F_c with environmental factors

The critical supporting area, A_c, of an observed stream network of a catchment shows spatial variation within the catchment (Figure 9 shows the distributions for five sample catchments); therefore, the mean value of a catchment is used for the correlation analysis. The mean A_c for the observed river networks is correlated with environmental factors, i.e., vegetation cover, topography and climate. The correlation with vegetation cover is stronger than that of topography and climate. The mean

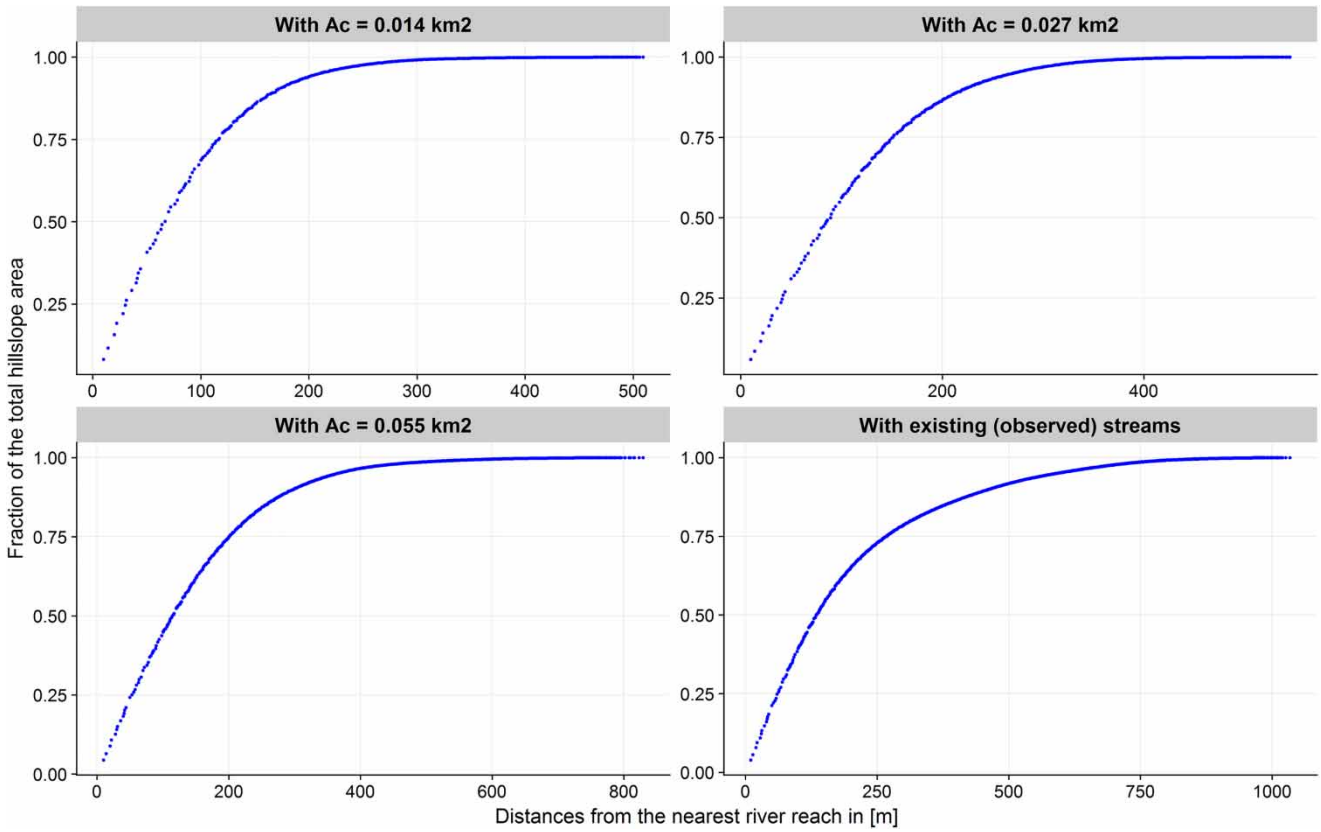

Figure 5 | Cumulative distance distributions functions of the dynamic hillslope distance distributions of Figure 4 for catchment 73.27.

A_c has a positive correlation with the forest cover in a catchment, but it has a negative correlation with mean annual precipitation, bare mountain cover and mean hillslope slope of a catchment. Table 8 shows the correlation between the mean A_c and F_c and the environmental factors.

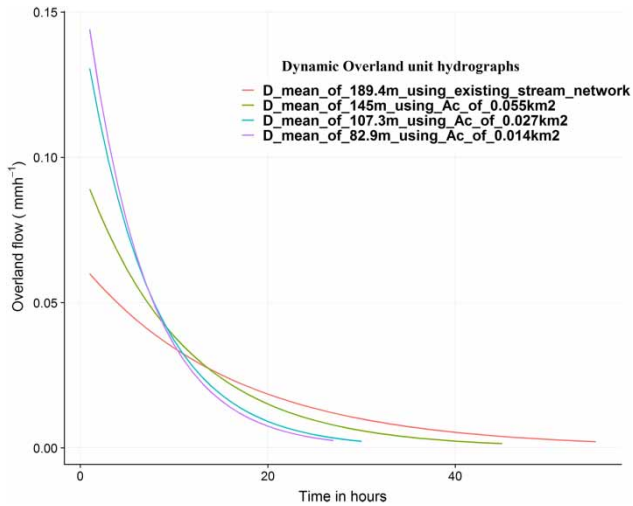

Figure 6 | Dynamic overland unit hydrographs of the cumulative distance distributions functions under Figure 5 during a flooding event for catchment 73.27.

The calibrated critical flux, F_c, of the dynamic river network routine is correlated with the environmental factors. The correlation between F_c and the vegetation cover is stronger than the correlation between F_c and topography and mean annual precipitation. F_c shows positive correlation with forest and negative correlation with bare mountain, mean annual precipitation and mean hillslope slope of a catchment. Table 9 shows the environmental factors used in the correlation analysis, the D_m and mean A_c of observed river network and the calibrated F_c of the dynamic river network routine of the study catchments.

The result of stepwise multiple linear regression shows that there is a potential to estimate F_c from the environmental factors as shown in Equation (17). Bare mountain is the only environmental factor contributing significantly to the regression with a significant level of 0.1. The multiple

Table 6 | Dynamic mean distance of the hillslope distance distributions estimated and used for generating dynamic overland unit hydrograph during flooding event at catchment 12.193 with a calibrated critical flux of 90 m^3/h

OF (mm/h)	A_c (m^2)	D_m (m) estimated using Equation (3)	D_m (m) used in deriving OUH
0.144	1,319,444.4	429.08	*301.1*
2.19	86,758	137.58	137.58
2.22	85,585.6	136.79	136.79
0.94	202,127.7	196.26	196.26
10.9	17,431.2	70.12	70.12
1.4	135,714.3	166.02	166.02
2.7	70,370.4	126	126
1.19	159,663.9	177.75	177.75
0.19	1,027,027	388.44	*301.1*
1.27	149,606.3	172.96	172.96
0.2	950,000	375.93	*301.1*
1.33	142,857.1	169.64	169.64
1.28	148,902.8	172.61	172.61
0.17	1,117,647.1	402.48	*301.1*
0.14	1,319,444.4	431.54	*301.1*
0.64	296,875	230.64	230.64
0.34	558,823.5	302	*301.1*
0.31	612,903.2	312.72	*301.1*
0.83	228,915.7	206.79	206.79

Italic numbers are rounded to two significant figures.

coefficient of determination (R^2) of the multiple regression is 0.3 and the significant level (P) is 0.06.

$$F_c\ (m^3/h) = 160.7 - 1.4 * \text{bare mountain}\ (\%) \quad (17)$$

DISCUSSION

Dynamic river networks

Dynamic river networks and hence dynamic OUHs are introduced and implemented in the DDD rainfall-runoff model to improve the simulation of floods. The dynamic river network method expands the observed river networks during OF events. The expansion means that the A_c required to initiate and maintain a stream decrease. Smaller A_c results in smaller D_m (see Table 5). The smaller D_m value indicates shorter travel times from points in the catchment to the nearest river reach. The shorter travel time distribution generates OUHs with a higher peak and shorter scale for the hillslopes (Figure 6). The dynamic OUHs are superpositioned with the other four subsurface UHs of DDD to give a single dynamic UH of a catchment during flooding events. The results of the method are supported by the previous study of D'Odorico & Rigon (2003) who found that shorter hillslope distances result in shorter travel times and hence higher flood peaks. The smaller D_m results, obtained during the flooding events using the dynamic river network method, are also supported by the study of Humbert (1990) who found that a good correlation exists between the runoff coefficient of flooding events and D_d, and hence the D_m, for 45 French catchments. Lazzaro *et al.* (2015) also found that the variability of runoff due to higher D_d (lower D_m) creates a faster concentration of flow that implies shorter travel times and higher peak floods. The results in this study are also supported by the results of Lee *et al.* (2008) who found that a UH of a catchment is dynamic during different precipitation intensities, i.e., the higher the precipitation intensity, the higher the peak and shorter the temporal scale of the UHs. The results of this study also show that a dynamic river network method could be a solution for rainfall-runoff models which face challenges in predicting flood peaks through continuous simulation. Improving the prediction of peak floods in a continuous simulation is very important because the hydrograph consisting of this peak flow is mainly responsible for the damage caused by floods. Therefore, a dynamic river network is a method to be conceptualized and included as one routine in continuous rainfall-runoff models which underestimate predictions of floods.

We analyzed statistically 91 underestimated flood peaks to evaluate the performance of the dynamic river network. The MARE and quantiles of RE of the prediction with and without dynamic river network show that the overall performance of the method has improved the prediction of the peaks satisfactorily. The dynamic river network overestimated 17 of the 91 flood peaks and still underestimates the remaining 74 floods but with a significant improvement in the prediction of flood peaks compared to the results obtained without a dynamic river network.

A single calibrated critical flux, F_c, improves the prediction of several underestimated floods significantly, but it also

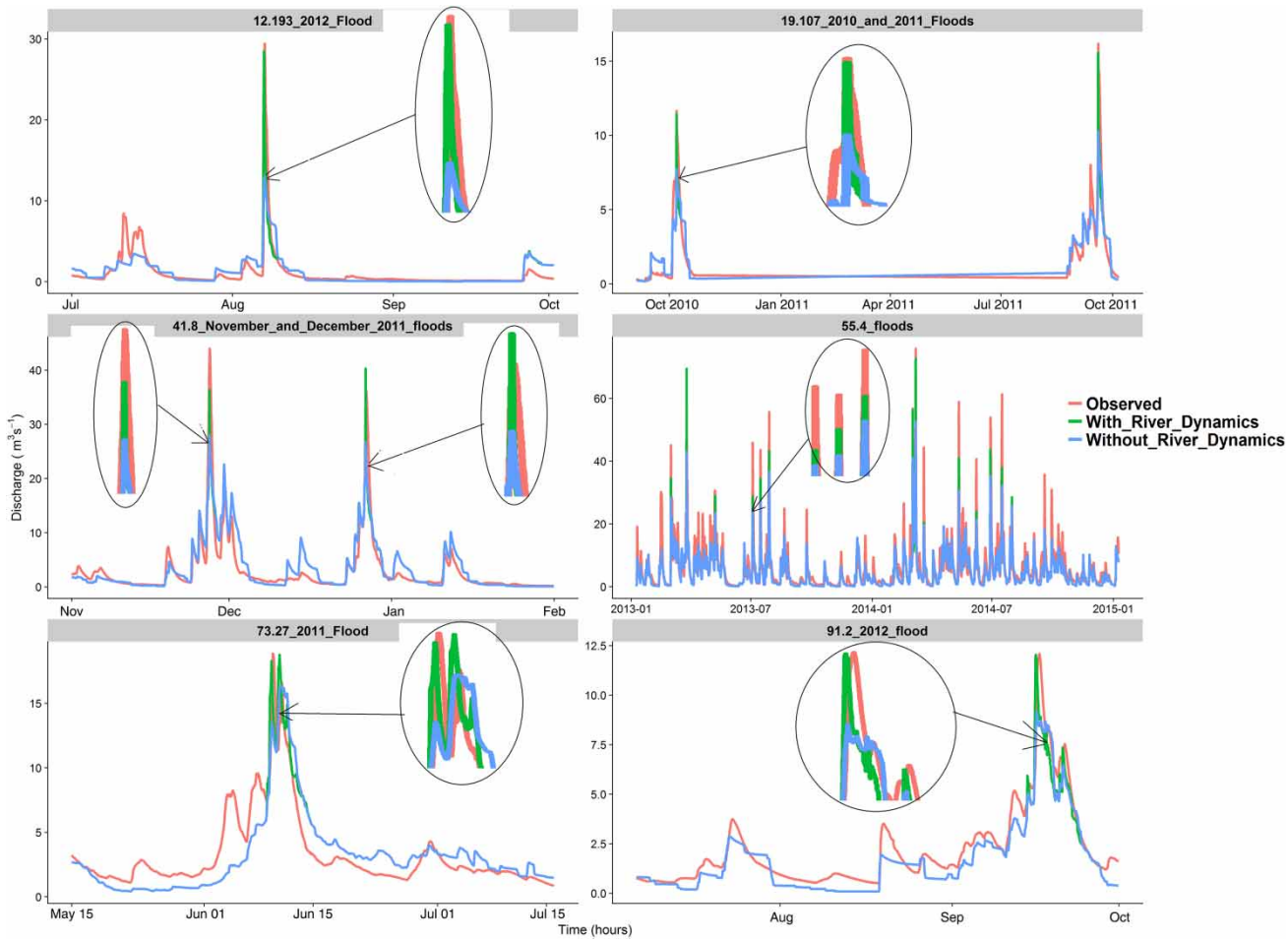

Figure 7 | Hydrographs of continuous simulations results of DDD rainfall-runoff models with flood peaks, i.e. observed, simulated with and without dynamic river network.

Table 7 | Observed and simulated floods using DDD with and without dynamic river network and the corresponding performance of the model for five sample catchments

Cat_ID	Observed flood(s) in m^3/s	Simulation period	Simulated value(s) of flood without river dynamics in m^3/s	Performance of DDD model without river dynamics in calibration		Simulated value(s) of flood with river dynamics in m^3/s	Performance of DDD model with river dynamics	
				KGE	BIAS		KGE	BIAS
12.193	*29.42*	2 years	*12.97*	0.64	1.2	*28.78*	0.65	1.2
19.107	*11.65* and *16.2*	3 years	*7.64* and *10.3*	0.8	0.93	*9.42* and *16.1*	0.81	0.94
41.8	*43.96* and *36.13*	2 years	*28.02* and *26.74*	0.77	0.84	*36.3* and *40.3*	0.77	0.84
73.27	*18.85*	3 years	*13.3*	0.71	0.76	*18.3*	0.71	0.76
91.2	*12.06*	2 years	*8.34*	0.71	0.8	*12.04*	0.71	0.8

Italic numbers are rounded to two significant figures.

overestimates a few flood peaks (Figure 7). Reasons for overestimation could be that a single calibrated F_c could not represent the different precipitation patterns, overland flow patterns and initial conditions prior to flooding events.

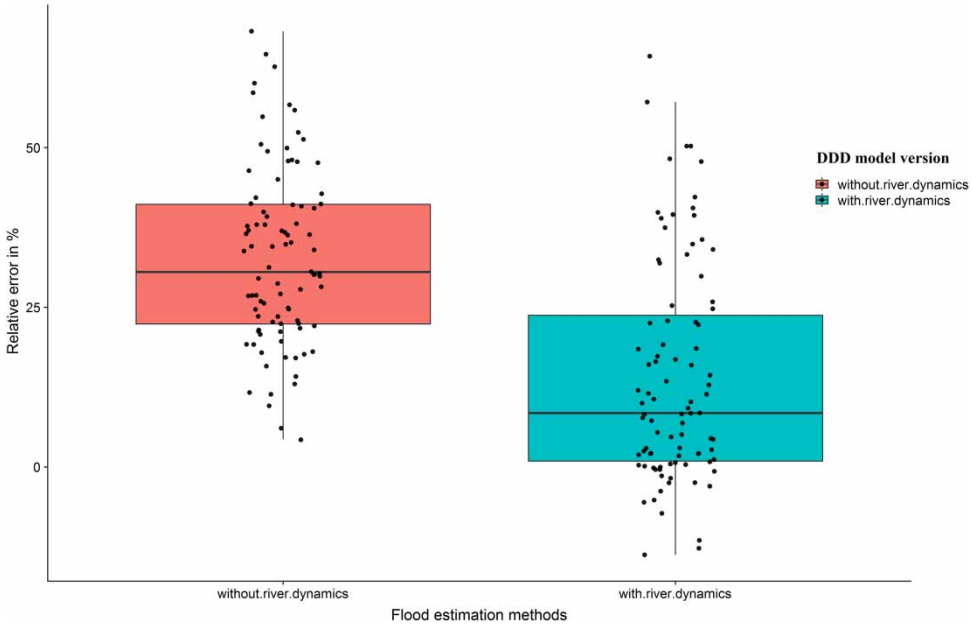

Figure 8 | Distributions of relative errors (%) of prediction of 91 flood peaks with and without dynamic river network.

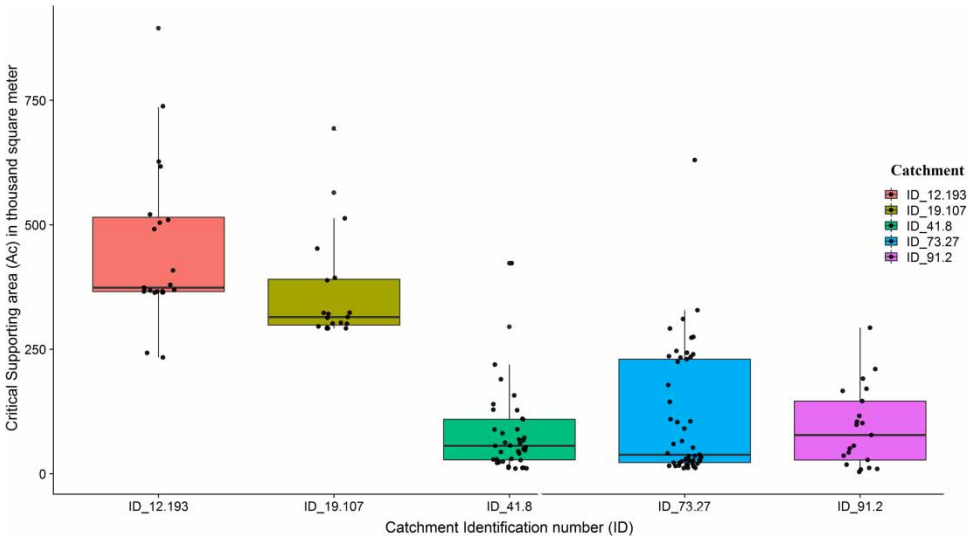

Figure 9 | Distributions of critical supporting area, i.e., A_c of observed stream networks for five of sample study catchments.

Table 8 | Correlation between calibrated critical flux, F_c of the dynamic river network with environmental variables, and correlation between mean critical area, A_c of the observed river network with some environmental variables

	Forest (%)	Bare mountain (%)	Mean hillslope slope (%)	Mean annual precipitation (mm)
Mean A_c (m^2)	0.63	−0.63	−0.56	−0.49
F_c (m^3/h)	0.46	−0.5	−0.29	−0.18

Another reason for such overestimation could be that the dynamic D_m estimated using Equation (3) is not always an accurate representation of the reality during a flood event. The limitations of manual calibration include subjectivity and time consuming. Manual calibration methods are subjective in the evaluation of model fit and the final choice of optimal parameters. Ndiritu (2009) pointed out that

Table 9 | The environmental factors used in the correlation analysis, the mean distance distribution, and mean critical area, A_c of observed river network, and the calibrated critical flux, F_c of the dynamic river network routine

	Environmental factors				Observed river network		
Cat_ID	Forest (%)	Bare mountain (%)	Mean annual precipitation (mm)	Mean hillslope slope (%)	D_m (m)	Mean A_c (m^2)	Dynamic river network F_c (m^3/h)
6.1	94.3	0	886	18.3	149.2	92,406	15
12.193	88.4	0	840	15.3	301.1	560,042	190
19.107	86.4	0	1,158	14.7	336.9	689,123	370
26.64	38.8	46.2	1,688	28.3	181.6	146,146	5
36.32	13.5	81.4	2,377	34.1	168.6	135,213	120
41.8	8.8	82.2	2,955	37.5	157.2	53,418	15
42.2	40.7	52.1	2,361	40.4	175.9	117,477	30
55.4	51.8	30.7	2,593	41.9	155.1	76,715	15
63.12	5.8	86.1	2,579	34.4	181.2	93,596	80
68.2	20.2	50.3	2,736	43.6	211.3	75,573	150
73.21	2.2	88	946	21.5	298.4	216,464	15
73.27	0.1	89.4	679	14.8	189.4	100,964	60
91.2	3.7	66.5	2,072	29.9	283.8	137,481	90
101.1	61.3	11.3	1,704	23.9	334.0	328,354	150
172.8	1.4	82.5	1,465	17	168.1	95,972	10

manual calibration may be more prone to obtaining suboptimal parameter sets than automatic calibration. Studies also show that manual calibration is more subjective than automatic calibration because it largely depends on visual hydrograph inspection and the personal judgment of the hydrologist. Substantial amount of time is also required to adjust F_c so that the observed and simulated flood peaks agreed well. A separate automatic calibration of F_c (which is not included in this study) after defining and writing appropriate objective function could improve the limitations of the manual calibration. However, since we have only one manually calibrated parameter and we have enough experience of using DDD model, the manual calibration result of F_c could be very good. In addition, the results of our study show that the manually calibrated F_c resulted in a significant improvement in predicting flood peaks using dynamic river network method.

The hydrograph in Figure 7 shows that the two floods of the catchment 41.8 could not be estimated well using a single calibrated F_c of magnitude 15 m^3/h even if the overall prediction of the flood peaks is improved. When we look at the flood hydrographs, the 27 November flood of 43.96 m^3/s (at 8 A.M), had been preceded by a 1-day precipitation of 68.9 mm (from 26 November 2011 09:00 to 27 November 2011 08:00). The precipitation was again preceded by a 3-day precipitation of magnitude 86.1 mm, i.e., the 4-day precipitation preceded the flooding event was 154.9 mm. When F_c is fitted to this single flooding event, 5 m^3/h is required. After 1 month, another heavy precipitation event happened (56.9 mm/day) and the event was preceded by 82.2 mm of 3-day precipitation, i.e., the 4-day precipitation preceded the flooding event was 139.7 mm. The magnitude of the flood was 36.13 m^3/s. When F_c is fitted to this single flooding event, 25 m^3/h is required. The variation in the fitted values of F_c for different flooding events in a catchment shows that we could have an overestimation of flooding events when we use a single calibrated F_c for the whole simulation period as a representative for a catchment. Accordingly, a single F_c of 15 m^3/h for the catchment 41.8 has overestimated the December 2011 flood, i.e., 36.13 m^3/s, but it has improved the overall prediction of the flood peaks in the catchment.

The spatial variability of A_c during flooding events, which is not considered in this study, could also be another

factor for the overestimation of floods using a single calibration value of F_c for a catchment. We have derived the coefficients of Equation (3) (a and b) with the assumption of constant A_c using the DEM, which considers only the topography of a catchment. However, the A_c of observed stream networks clearly shows that there is a spatial variability of A_c within a catchment. Geological and land use factors play significant roles in initiating and maintaining a stream, and these factors control the spatial variability of A_c in a catchment (Montgomery & Dietrich 1989; Ogden *et al.* 2011; Sjöberg 2016; Ward *et al.* 2018) in addition to the topography. The correlation results between A_c and vegetation cover, which is done in this study and explained in the next section, also confirm that the land use affects the spatial variability of A_c. Figure 7 shows box plots of the spatial distributions of A_c of observed stream network for five sample catchments. For flooding events preceded by short duration and higher values of OF, Equation (3) gives very low values of D_m. The very low D_m gives OUHs of sharp peak and short scales which overestimated the floods. However, if we had calculated the actual D_m using the spatial variability of A_c, we could have found higher values of D_m than the value calculated using Equation (3) and the overestimation could have been avoided.

For estimating the parameters of travel time distributions of overland flow of a hillslope, we followed the original approach used in DDD (e.g. the distance from any point in the catchment to the nearest river network is calculated using the Euclidean distance and the celerity is determined from recession analysis). The GIUH and of width function estimates the distribution of travel times at the outlet of a catchment combining the hillslope and river network travel times using the steepest descent path from any point in the catchment to the outlet and the shape and scale parameters of the travel time distribution could change with the extent of hillslope saturation. Therefore, further investigation, i.e., comparison assessment is required before concluding as one method is better than the other.

Correlation of A_c and F_c with environmental factors

Environmental factors such as vegetation cover, topography and climate, affect A_c and hence D_m. Land use (e.g. vegetation cover) affects the hydrology and can affect subsurface as well as overland flow which in turn can cause changes in the stream network, i.e., A_c (Jonathan & Dennis 2001). The correlation results show that the denser the vegetation cover in a catchment the higher the A_c is required for initiating and maintaining a stream and vice versa, i.e., positive correlation with forest and negative correlation with bare mountain. The correlation result confirms the findings that a decrease in vegetation causes a decrease in surface resistance and critical shear stress, which result in an increase of drainage density (a reduction in D_m), i.e., streams form easier in less vegetated catchments (Willgoose *et al.* 1991; Prosser & Dietrich 1995; Magnuson *et al.* 1997; Tucker & Slingerland 1997). Field observations also show that higher D_m and hence higher A_c is generally observed in denser vegetation cover (Morisawa 1985).

The steepness of a catchment is one of the topographical factors controlling A_c and hence D_m. In this study, we used the mean hillslope slope of a catchment and found that a catchment hillslope slope has negative correlation with A_c, i.e., the higher the steepness, the lower the A_c required to initiate and maintain stream. This finding is supported by Montgomery & Dietrich (1989) who found that stream initiation on steep slopes shows a negative relationship between valley gradient at the stream head and A_c, i.e., the higher the stream head slope the lower the A_c (lower D_m).

The positive correlation between F_c and vegetation cover in a catchment shows that the denser the vegetation covers, the higher the F_c. F_c shows negative correlation with bare mountain, mean hillslope slope and mean annual precipitation of a catchment. The A_c and hence F_c depend on several factors, which include geology, precipitation, vegetation, morphology, soils and land uses, and one factor may be more important than another (see Table 8). Therefore, a more detailed investigation supported by field work (e.g. mapping of the slope, geology, vegetation cover and soil of a catchment at the head of first-order streams of observed river networks and mapping of the pattern of expansion of first-order streams during flooding events) should be carried out to assess how the combination of these factors control A_c and hence F_c.

We have done a simple multiple linear regression analysis using the four environmental factors as predictors, i.e., forest, bare mountain, slope and mean annual precipitation,

to estimate the response variable F_c. The result shows that only bare mountain is contributing significantly in estimating F_c with a significance level of 0.1, and the coefficient of determination of the regression (R^2) is 0.3. The objective of the regression analysis, done in this study, is to assess a preliminary method for regionalization that can predict F_c for ungauged catchments from environmental factors and to lay a foundation for further studies.

A dynamic river network method could be implemented in rainfall-runoff models as shown for DDD for prediction of floods for catchments with a wide range of topography and land uses (Table 1). In this study, the effect of steep hills is reflected in the dynamic river networks as the steepness of a catchment is one of the factors that govern the initiation of streams. As shown in Table 8, the mean hillslope slope has a negative correlation with A_c, i.e., we need a smaller A_c to initiate and maintain streams in steep topography than in a flat topography. Table 9 also shows that the mean A_c of an observed stream network decreases as the mean hillslope slope of a catchment increases. The fundamental theory behind the method is the expansion of river networks during flooding events, i.e., whether the critical flux, F_c, which is required to initiate and maintain a stream, is satisfied or not. The magnitude of F_c depends on the magnitude of saturation excess overland flow, OF, and the critical support area, A_c. The study results also show that the critical support area, required to initiate and maintain a stream, is smaller in steep and bare mountain catchments than flat and forested catchments. Therefore, the method could be applicable at different catchments with different characteristics.

CONCLUSIONS

The dynamic river network method, introduced in Distance Distribution Dynamics (DDD) rainfall-runoff model, can improve the prediction of flood peaks in continuous simulation satisfactorily. The performance of the DDD model is the same with and without dynamic river network in terms of KGE and BIAS. The statistical analysis on 91 flood peaks, underestimated by DDD without dynamic river network method, shows that the MARE of the prediction reduced from 32.9% to 15.7% using the dynamic river network method. With a dynamic river network method, the 0.75 quantile of the relative errors reduced from 41% to 23%, and the 0.25 quantile of the relative errors reduced from 22% to 1%. The visual inspection of the hydrographs also shows an improvement in the prediction of flood peaks for several flooding events. Therefore, we recommend the use of a dynamic river network method in the prediction of floods. The next step in the development of the method is to investigate the applicability of the method from gauged to ungauged catchments and find a way to address the limitations identified in this study.

The critical flux, F_c, the calibration parameter introduced in the method, has been formulated as the product of critical supporting area (A_c) and the saturated excess overland flow (OF). F_c shows stronger correlation with vegetation cover than topographical and climate factors. The parameter shows positive correlation with forest cover of catchments, and negative correlation with bare mountain, mean hillslope slope and mean annual precipitation. The simple multiple linear regression, using the four environmental factors as predictors and F_c as a response variable, shows that there is a potential to estimate F_c from environmental factors and regionalize it for using the method without calibration. The value of the calibrated F_c could be different for the same catchment of different flood magnitudes, and it could be different for the same type of vegetation cover for different catchments. This difference shows that F_c could depend on several environmental factors and further investigations should be carried out.

ACKNOWLEDGEMENTS

The authors would like to acknowledge Cristian Lussana of the Norwegian Meteorological Institute for providing information on how to access and process the 1×1 km spatial and 1-h temporal resolution gridded precipitation and temperature data for Norway. Finally, the authors gratefully acknowledge the financial support by the Research Council of Norway and several partners through the Centre for Research-based Innovation 'Klima 2050' (see www.klima2050.no).

REFERENCES

Bencala, K. E., Gooseff, M. N. & Kimball, B. A. 2011 Rethinking hyporheic flow and transient storage to advance understanding of stream-catchment connections. *Water Resources Research* **47**, 3. doi:10.1029/2010WR010066.

Bergström, S. 1976 *Development and Application of a Conceptual Runoff Model for Scandinavian Catchments*. Department of Water Resources Engineering, Lund Institute of Technology, University of Lund, Lund.

Beven, K. 2001b *Rainfall-Runoff Modelling: The Primer*. John Wiley and Sons, Chichester, UK, pp. 1–360.

Blaikie, P., Cannon, T., Davis, I. & Wisner, B. 2014 *At Risk: Natural Hazards, People's Vulnerability and Disasters*. Routledge, London.

Blazkova, S. & Beven, K. 2002 Flood frequency estimation by continuous simulation for a catchment treated as ungauged (with uncertainty). *Water Resources Research* **38** (8), 14-11–14-14. doi:10.1029/2001WR000500.

Boughton, W. & Droop, O. 2003 Continuous simulation for design flood estimation – a review. *Environmental Modelling & Software* **18**, 309–318. https://doi.org/10.1016/S1364-8152(03)00004-5.

Bourdin, D. R., Fleming, S. W. & Stull, R. B. 2012 Streamflow modelling: a primer on applications, approaches and challenges. *Atmosphere-Ocean* **50** (4), 507–536. doi:10.1080/07055900.2012.734276.

Bras, R. L. 1990 *Hydrology: An Introduction to Hydrologic Science*. Addison-Wesley, Reading, MA.

Brocca, L., Melone, F. & Moramarco, T. 2011 Distributed rainfall-runoff modelling for flood frequency estimation and flood forecasting. *Hydrological Processes* **25** (18), 2801–2813. doi:10.1002/hyp.8042.

Calver, A. & Lamb, R. 1995 Flood frequency estimation using continuous rainfall-runoff modelling. *Physics and Chemistry of the Earth* **20** (5), 479–483. doi:10.1016/S0079-1946(96)00010-9.

Cameron, D., Beven, K., Ja, T. & Naden, P. 2000 Flood frequency estimation by continuous simulation (with likelihood based uncertainty estimation). *Hydology and Earth System Sciences* **4**, 23–34.

Camici, S., Tarpanelli, A., Brocca, L., Melone, F. & Moramarco, T. 2011 Design soil moisture estimation by comparing continuous and storm-based rainfall-runoff modeling. *Water Resources Research* **47**, 5. doi:10.1029/2010WR009298.

Chetty, K. & Smithers, J. 2005 Continuous simulation modelling for design flood estimation in South Africa: preliminary investigations in the Thukela Catchment. *Quarterly Journal of the Royal Meteorological Society* **30**, 3–23.

Chorley, R. J. & Morgan, M. A. 1962 Comparison of morphometric features, Unaka Mountains, Tennessee and North Carolina, and Dartmoor, England. *GSA Bulletin* **73** (1), 17–34. doi:10.1130/0016-7606(1962)73[17:COMFUM]2.0.CO;2.

Collier, C. G. 2007 Flash flood forecasting: what are the limits of predictability? *Quarterly Journal of the Royal Meteorological Society* **133** (622), 3–23. https://doi.org/10.1002/(SICI)1099-1085(19970630)11:8<825::AID-HYP509>3.0.CO;2-G.

Day, D. G. 1983 Drainage density variability and drainage basin outputs. *Journal of Hydrology (New Zealand)* **22** (1), 3–17.

Di Lazzaro, M., Zarlenga, A. & Volpi, E. 2014 A new approach to account for the spatial variability of drainage density in rainfall-runoff modelling. *Boletin Geologico y Minero* **125** (3), 301–313.

Dingman, S. L. 1978 Drainage density and streamflow: a closer look. *Water Resources Research* **14** (6), 1183–1187. doi:10.1029/WR014i006p01183.

D'Odorico, P. & Rigon, R. 2003 Hillslope and channel contributions to the hydrologic response. *Water Resources Research* **39**, 5. doi:10.1029/2002WR001708.

Dunne, T. 1978 Field studies of hillslope flow processes. In: *Hillslope Hydrology*, Vol. 9 (M. J. Kirkby ed.), *Geographical Research Letters* **9**, 227–293.

Eschenbach, D., Haberlandt, U., Buchwald, L. & Belli, A. 2008 Derived flood frequency analysis using rainfall runoff modelling and synthetic precipitation data. *Wasserwirtchaft* **98** (11), 19–23.

ESRI 2014 *ArcGISDesktop Help 10.3 Geostatistical Analyst*. https://www.esri.com/en-us/home.

Filipova, V., Lawrence, D. & Skaugen, T. 2018 A stochastic event-based approach for flood estimation in catchments with mixed rainfall/snowmelt flood regimes. *Natural Hazards and Earth System Sciences Discussion* **2018**, 1–30. doi:10.5194/nhess-2018-174.

Fleig, A. K. & Wilson, D. 2013 *Flood Estimation in Small Catchments: Literature StudyNaturfareprosjektet,Rapport (Norges Vassdrags-og Energidirektorat: Online) (Vol. no. 60-2013)*. Norwegian Water Resources and Energy Directorate, Oslo.

Formetta, G., Prosdocimi, I., Stewart, E. & Bell, V. 2017 Estimating the index flood with continuous hydrological models: an application in Great Britain. *Hydrology Research* **49**, 23–33.

Gao, H., Cai, H. & Duan, Z. 2017 Understanding the impacts of catchment characteristics on the shape of the storage capacity curve and its influence on flood flows. *Hydrology Research* **49** (1), 90–106. doi:10.2166/nh.2017.245.

Godsey, S. E. & Kirchner, J. W. 2014 Dynamic, discontinuous stream networks: hydrologically driven variations in active drainage density, flowing channels and stream order. *Hydrological Processes* **28** (23), 5791–5803. doi:10.1002/hyp.10310.

Gupta, V. K., Waymire, E. & Wang, C. T. 1980 A representation of an instantaneous unit hydrograph from geomorphology. *Water Resources Research* **16** (5), 855–862. doi:10.1029/WR016i005p00855.

Gupta, H. V., Kling, H., Yilmaz, K. K. & Martinez, G. F. 2009 Decomposition of the mean squared error and NSE performance criteria: implications for improving

hydrological modelling. *Journal of Hydrology* **377** (1), 80–91. doi:10.1016/j.jhydrol.2009.08.003.

Haberlandt, U. & Radtke, I. 2014 Hydrological model calibration for derived flood frequency analysis using stochastic rainfall and probability distributions of peak flows. *Hydrology and Earth System Sciences* **18** (1), 353–365. doi:10.5194/hess-18-353-2014.

Hirabayashi, Y., Mahendran, R., Koirala, S., Konoshima, L., Yamazaki, D., Watanabe, S. & Kanae, S. 2013 Global flood risk under climate change. *Nature Climate Change* **3**, 816. doi:10.1038/nclimate1911. https://www.nature.com/articles/nclimate1911#supplementary-information

Horton, R. E. 1932 Drainage-basin characteristics. *Eos, Transactions American Geophysical Union* **13** (1), 350–361. doi:10.1029/TR013i001p00350.

Horton, R. E. 1945 Erosional development of streams and their drainage basins: hydrophysical approach to quantitative morphology. Bulletin of the Geological Society of America 56, 275-370. *Progress in Physical Geography: Earth and Environment* **19** (4), 533–554. doi:10.1177/030913339501900406.

Humbert, J. 1990 Interet de la densite de drainage pour regionaliser les donnees hydrologiques en zone montagneuse. In: *Hydrology in Mountainous Regions I, Hydrological Measurements, the Water Cycle*. IAHS Publisher, Strasbourg, pp. 373–380.

Jonathan, L. L. M. & Dennis, P. L. 2001 Effects of forest roads on flood flows in the Deschutes river. *Earth Surface Processes and Landforms* **26**, 115–134, Vol. **26**. Washington.

Lamb, R. & Kay, A. L. 2004 Confidence intervals for a spatially generalized, continuous simulation flood frequency model for Great Britain. *Water Resources Research* **40** (7). doi:10.1029/2003WR002428.

Lazzaro, D. M., Zarlenga, A. & Volpi, E. 2015 Hydrological effects of within-catchment heterogeneity of drainage density. *Advances in Water Resources* **76**, 157–167. doi:10.1016/j.advwatres.2014.12.011.

Lee, K. T., Chen, N.-C. & Chung, Y.-R. 2008 Derivation of variable IUH corresponding to time-varying rainfall intensity during storms/Dérivation d'un HUI variable correspondant à l'évolution temporelle de l'intensité pluviométrique durant les averses. *Hydrological Sciences Journal* **53** (2), 323–337. doi:10.1623/hysj.53.2.323.

Lu, Q. & Han, Q.-L. 2011 A probability particle swarm optimizer with information-sharing mechanism for odor source localization. *IFAC Proceedings Volumes* **44** (1), 9440–9445. doi:10.3182/20110828-6-IT-1002.00507.

Lussana, C., Ole Einar, T. & Francesco, U. 2016 Senorge v2.0: an observational gridded dataset of temperature for Norway. *METreport* **108**, 75–86.

Magnuson, J., Webster, K., Assel, R., Bowser, C., Dillon, P., Eaton, J. & Mortsch, L. 1997 Potential effects of climate changes on aquatic systems: Laurentian Great Lakes and Precambrian Shield region. *Hydrological Processes* **11**. doi:10.1002/(SICI)10991085(19970630)11:8<825::AID-HYP509>3.3.CO;2-7.

Maidment, D. R. 1993 *Developing A Spatially Distributed Unit Hydrograph by Using GIS*. IAHS Publication, Austin, TX, 211, pp. 181–192.

Moglen, G. E., Eltahir, E. A. B. & Bras, R. L. 1998 On the sensitivity of drainage density to climate change. *Water Resources Research* **34** (4), 855–862. doi:10.1029/97WR02709.

Montgomery, D. R. & Dietrich, W. E. 1989 Source areas, drainage density, and channel initiation. *Water Resources Research* **25** (8), 1907–1918. doi:10.1029/WR025i008p01907.

Morisawa, M. 1985 *Rivers. Form and Process*. Longman Inc, New York.

Ndiritu, J. 2009 A comparison of automatic and manual calibration using the Pitman Model. *Engineering* **34**, 62–63.

Nhim, T. 2012 *Variability of Intermittent Headwater Streams in Boreal Landscape: Influence of Different Discharge Conditions. 248 Student Thesis*. Available from: http://urn.kb.se/resolve?urn=urn:nbn:se:uu:diva-183137; DiVA database.

Ogden, F. L., Raj Pradhan, N., Downer, C. W. & Zahner, J. A. 2011 Relative importance of impervious area, drainage density, width function, and subsurface storm drainage on flood runoff from an urbanized catchment. *Water Resources Research* **47** (12). doi:10.1029/2011WR010550.

Papageorgaki, I. & Nalbantis, I. 2017 Definition of critical support area revisited. *European Water* **57**, 273–278.

Pathiraja, S., Westra, S. & Sharma, A. 2012 Why continuous simulation? The role of antecedent moisture in design flood estimation. *Water Resources Research* **48**, 6. doi:10.1029/2011WR010997.

Plate, E. J. 2009 Classification of hydrological models for flood management. *Hydrology and Earth System Sciences* **13** (10), 12. doi:10.5194/hess-13-1939-2009.

Prosser, I. P. & Dietrich, W. E. 1995 Field experiments on erosion by overland flow and their implication for a digital terrain model of channel initiation. *Water Resources Research* **31** (11), 2867–2876. doi:10.1029/95WR02218.

Rahman, A., Hoang, T. M. T., Weinmann, P. E. & Laurenson, E. M. 1998 *Joint Probability Approaches to Design Flood Estimation: A Review Report 98/8*. CRC for Catchment Hydrology, Clayton, VIC.

Razi, M., Ariffin, J., Tahir, W. & Arish, N. A. M. 2010 Flood estimation studies using hydrologic modeling system (HEC-HMS) for Johor river. *Journal of Applied Sciences* **10**, 930–939. doi:10.3923/jas.2010.930.939.

R Core Team 2017 *R: A Language and Environment for Statistical Computing*. Available from: http://www.R-project.org/

Reis, D. S. & Stedinger, J. R. 2005 Bayesian MCMC flood frequency analysis with historical information. *Journal of Hydrology* **313** (1), 97–116. doi:10.1016/j.jhydrol.2005.02.028.

Rigon, R., D'Odorico, P. & Bertoldi, G. 2011 The geomorphic structure of the runoff peak. *Hydrology and Earth System Sciences* **15** (6), 1853–1863. doi:10.5194/hess-15-1853-2011.

Rinaldo, A., Marani, A. & Rigon, R. 1991 Geomorphological dispersion. *Water Resources Research* **27** (4), 513–525.

Rinaldo, A., Vogel, G. K., Rigon, R. & Rodriguez-Iturbe, I. 1995 Can one gauge the shape of a basin? *Water Resources Research* **31** (4), 1119–1127. doi:10.1029/94WR03290.

Robinson, J. S., Sivapalan, M. & Snell, J. D. 1995 On the relative roles of hillslope processes, channel routing, and network geomorphology in the hydrologic response of natural catchments. *Water Resources Research* **31** (12), 3089–3101. doi:10.1029/95WR01948.

Rodríguez-Iturbe, I. & Valdés, J. B. 1979 The geomorphologic structure of hydrologic response. *Water Resources Research* **15** (6), 1409–1420. doi:10.1029/WR015i006p01409.

Rusjan, S., Kobold, M. & Mikoš, M. 2009 Characteristics of the extreme rainfall event and consequent flash floods in W Slovenia in September 2007. *Natural Hazards and Earth System Sciences* **9**, 3. doi:10.5194/nhess-9-947-2009.

Schaefer, M., Elifrits, D. & Barr, D. 1979 *Sculpturing Reclaimed Land to Decrease Erosion, Paper Presented at the Symposium on Surface Mining Hydrology, Sedimentology and Reclamation*. University of Lexington, Kentucky.

Singh, V. P. 1995 *Computer Models of Watershed Hydrology*. Water Resources Publications, Littleton, CO.

Singh, V. P. & Frevert, D. K. 2006 Watershed models. *Experimental Agriculture* **42** (3), 370. doi:10.1017/S0014479706293797.

Sjöberg, O. 2016 *The Origin of Streams: Stream Cartography in Swiss Pre Alpine Headwater. 16003 Student Thesis*. Available from: http://urn.kb.se/resolve?urn=urn:nbn:se:uu:diva-277377 DiVA database.

Skaugen, T. & Mengistu, Z. 2016 Estimating catchment-scale groundwater dynamics from recession analysis – enhanced constraining of hydrological models. *Hydrology and Earth System Sciences* **20** (12), 4963–4981. doi:10.5194/hess-20-4963-2016.

Skaugen, T. & Onof, C. 2014 A rainfall-runoff model parameterized from GIS and runoff data. *Hydrological Processes* **28** (15), 4529–4542. doi:10.1002/hyp.9968.

Skaugen, T. & Weltzien, I. H. 2016 A model for the spatial distribution of snow water equivalent parameterized from the spatial variability of precipitation. *The Cryosphere* **10** (5), 1947. doi:10.5194/tc-10-1947-2016.

Skaugen, T., Peerebom, I. O. & Nilsson, A. 2015 Use of a parsimonious rainfall–run-off model for predicting hydrological response in ungauged basins. *Hydrological Processes* **29** (8), 1999–2013. doi:10.1002/hyp.10315.

Smithers, J. 2012 Methods for design flood estimation in South Africa. *Water SA* **38**, 633–646.

Smithers, J., Chetty, K., Frezghi, M., Knoesen, D. & Tewolde, M. 2013 Development and assessment of a daily time-step continuous simulation modelling approach for design flood estimation at ungauged locations: ACRU model and Thukela Catchment case study. *Water SA* **39**, 00–00.

Thiemig, V., Rojas, R., Zambrano-Bigiarini, M. & De Roo, A. 2013 Hydrological evaluation of satellite-based rainfall estimates over the Volta and Baro-Akobo Basin. *Journal of Hydrology* **499**, 324–338. doi:10.1016/j.jhydrol.2013.07.012.

Thomas, W. O. 1982 An evaluation of flood frequency estimates based on rainfall/runoff modeling1. *JAWRA Journal of the American Water Resources Association* **18** (2), 221–229. doi:10.1111/j.1752-1688.1982.tb03964.x.

Tsegaw, A. T., Alfredsen, K., Skaugen, T. & Muthanna, T. M. 2019 Predicting hourly flows at ungauged small rural catchments using a parsimonious hydrological model. *Journal of Hydrology*. doi:10.1016/j.jhydrol.2019.03.090.

Tucker, G. E. & Slingerland, R. 1997 Drainage basin responses to climate change. *Water Resources Research* **33** (8), 2031–2047. doi:10.1029/97WR00409.

Tucker, G. E., Catani, F., Rinaldo, A. & Bras, R. L. 2001 Statistical analysis of drainage density from digital terrain data. *Geomorphology* **36** (3), 187–202. doi:10.1016/S0169-555X(00)00056-8.

Ward, A. S., Schmadel, N. M. & Wondzell, S. M. 2018 Simulation of dynamic expansion, contraction, and connectivity in a mountain stream network. *Advances in Water Resources* **114**, 64–82. doi:10.1016/j.advwatres.2018.01.018.

Wharton, G. 1994 Progress in the use of drainage network indices for rainfall-runoff modelling and runoff prediction. *Progress in Physical Geography: Earth and Environment* **18** (4), 539–557. doi:10.1177/030913339401800404.

Willgoose, G., Bras, R. L. & Rodriguez-Iturbe, I. 1991 A coupled channel network growth and hillslope evolution model: 1. Theory. *Water Resources Research* **27** (7), 1671–1684. doi:10.1029/91WR00935.

Winsemius, H., Aerts, J., van Beek, L. P. H., Bierkens, M. F. P., Bouwman, A., Jongman, B. & Ward, P. 2015 Global drivers of future river flood risk. *Nature Climate Change* **6**, 381–385.

First received 19 December 2018; accepted in revised form 5 July 2019. Available online 26 August 2019